DEEP NEURAL NETWORKS AS A TOOL TO ESTIMATION OF COSMIC RADIATION DOSE RECEIVED ON FLIGHT

Ayberk YILMAZ[1], Hatice YILMAZ ALAN[2], Özlem FAYDASIÇOK[3], Lidya AMON SUSAM[4], Rüya ŞAMLI[5], Baki AKKUŞ[6], Aydın EROL[7], Ertan GÜDEKLİ[8], Çisem İlayda İNCİ[9], Mehmet Erhan EMİRHAN[10]

Cosmic radiation is an ionizing radiation produced when primary protons and α particles from outside the solar system interact with components of the earth's atmosphere. Cosmic radiation is a general term for radiation produced by high-energy subatomic particles from outer space and, more importantly, secondary (ionizing) radiation from the sun and high-energy subatomic particles that react with nitrogen, oxygen, and other elements in the atmosphere. In this study, Deep Neural Networks (DNNs) via Multilayer Perceptrons (MLPs) were used to estimate the radiation doses due to cosmic radiation for different domestic flights related with Istanbul and Ankara Airports in Turkey. Dose values were calculated with the CARI-7A program and DNNs. The parameters for calculating dose rates are latitude, longitude and depth. The results obtained compared and discussed.

Keywords: aircrew, cosmic radiation, flight, machine learning, deep learning, multilayer perceptrons.

1. Introduction

The Cosmic radiation term was known as radiation from space [1,2]. Cosmic rays with high-energy move through space and most of them sooner or

[1] Corresponding author, Assoc. Prof. Dr, Dept.of Physics, Faculty of Science, Istanbul University, Turkey, e-mail: ayberk@istanbul.edu.tr
[2] Instructor. Dr, Institute of Accelerator Technologies, Ankara University, Ankara, Turkey, e-mail: hyalan@ankara.edu.tr.
[3] Asst. Prof. Dr, Dept. of Mathematics, Faculty of Science, Istanbul University, Istanbul, Turkey, e-mail: kozlem@istanbul.edu.tr
[4] Assoc. Prof. Dr, Dept. of Physics, Faculty of Science, Istanbul University, Turkey, e-mail: lidyamon@istanbul.edu.tr
[5] Prof. Dr, Department of Computer Engineering, Istanbul University-Cerrahpasa, Istanbul, Turkey, e-mail: ruyasamli@iuc.edu.tr
[6] Prof. Dr, Dept. of Physics, Faculty of Science, Istanbul University, Turkey, e-mail: akkus@istanbul.edu.tr
[7] Graduate Student, Dept. of Physics, Yıldız Technical University-Davutpasa, Turkey, e-mail:
[8] Assoc. Prof. Dr, Dept. of Physics, Faculty of Science, Istanbul University, Turkey, e-mail: gudekli@istanbul.edu.tr
[9] Student, Dept. of Physics, Faculty of Science, Istanbul University, Turkey, e-mail: cisemilaydainci@gmail.com
[10] Instructor. Dr, Dept. of Physics, Faculty of Science, Istanbul University, Turkey, e-mail: mehmet.emirhan@istanbul.edu.tr

later reaches the Earth's surface. They travel nearly at the speed of light. Galactic and solar are two kinds of cosmic rays. The remnants of supernovas shown the reason of galactic cosmic rays and by the powerful explosions of massive stars at the last stages charged particles accelerated and Earth exposed to these radiations all the time. One other kind is the solar cosmic radiation where electrons, protons and helium nuclei emitted from the Sun in two ways either from solar wind or from magnetic fields on the Sun's surface. As it is known The Earth shielded by a magnetic field and mainly most of these radiations caused by galactic and solar based bounce from the poles. But some of these cosmic radiations still manage to reach the Earth and exposed by people. Averagely, people are exposed to around 3.5 mSv of radiation per year [1,3,4] where only 10% of this amount comes from cosmic radiation. Airplane passengers are exposed to high levels of cosmic radiation [2,5] during a flight at higher altitudes, latitudes and especially if they fly too frequently or fly longer destinations. That's why there are many programs [6] written to calculate the total cosmic dose received during a flight. These programs [3,6] are mainly used for aircrew not to cause high levels of cosmic dose and this is one of the top majority safety standards to keep them healthy. Up until now the programs such as AVIDOS, CARI-7, EPCARD.Net, FDOScalc, JISCARD, PANDOCA, PCAIRE, EXPACS, and SIEVERT [3,6,7,8,9,10,11,12,13,14] coded were based on mostly Monte Carlo simulation techniques, or some analytical solutions or semi-empirical measurements. There are publications where these methods used to calculate the exposed cosmic dose on flight for different destinations [15-19]. In this publication, Deep Neural Networks (DNNs) via Multilayer Perceptrons (MLPs) were used to estimate the cosmic radiation doses for different domestic flights related with Istanbul and Ankara Airports in Turkey. Besides DNNs, just to make a correct comparison in between, a well-known program CARI-7A [8] is used to calculate the dose values as well. The parameters used for calculating dose rates are latitude, longitude, and depth. The results obtained from this work is compared and discussed in the following.

2. Methods and theoretical calculations

In this study, the cosmic radiation dose received during flights was calculated using the CARI-7A program. The estimated value of this dose was obtained by means of machine learning method (MLPs).

2.1 Calculation of dose at aviation altitudes by CARI7-A

The received cosmic radiation dose (effective dose) for any flight vary with latitude, longitude and altitude. Various models have been developed to calculate the Cosmic radiation dose in aviation [20]. The computer program

CARI-7A, developed by the Federal Aviation Administration's (FAA's) Civil Aviation and Space Medical Institute, calculates the effective dose of galactic cosmic radiation by a crewmember or the passengers can be calculated [21]. CARI-7A calculates the theorical cosmic radiation dose (effective dose), taking into account flight route information, flight time, altitude and position (latitude and longitude). The program takes into account solar activity and the effects of geomagnetic field on galactic cosmic radiation levels for the user-selected date. The heliocentric potential is used for the precise calculation, thereby allowing the program to adjust for changes in galactic radiation levels that occur with changes in solar activity. In the calculations, heliocentric potential (HP) modulated ISO local interstellar GCR spectrum (LIS) was used for the GCR model [22-25]. Radiation dose calculated in μSv unit according to ICRP Pub.103 effective dose [26].

2.2 Machine learning and Scikit-Learn

Machine Learning is an artificial intelligence application in which methods that make inferences from existing data using mathematical and statistical methods and make predictions about the unknown with these inferences are developed. Machine learning teaches computers to think and act like humans, and to improve their performance by making decisions with appropriate data and algorithms for new applications similar to applications that computers have experienced before, with minimal human intervention [27-29]. Scikit-learn is a Python-based library used to build machine learning models. This library focuses on machine learning tools including mathematical, statistical and general-purpose algorithms [30]. It contains many learning algorithms for machine learning tasks that include classification, regression, dimensionality reduction, and clustering. It also provides modules to extract features, manipulate data, and evaluate models. It is compatible with NumPy and SciPy and it can easily work with different Python libraries. NumPy extends Python to support efficient operations on large arrays and multidimensional matrices [31]. Matplotlib provides modules for visualization tools [32] and SciPy provides modules for scientific calculations [33]. Scikit-learn is licensed under a simplified BSD license and is distributed under many Linux distributions that encourage academic and commercial use.

2.3 Artificial neural network (ANN), multi-layer perceptrons (MLPs) and deep neural network (DNN)

Artificial intelligence has been defined in the scientific world as the ability of a computer or a computer-aided machine to perform tasks related to higher logical processes, usually human qualities (finding a solution, learning from the past experiences and generalization) [34]. Artificial intelligence technologies

consist of expert systems, fuzzy logic artificial, neural networks, machine learning and genetic algorithms. In machine learning, relationships between inputs and outputs of events are usually learned using examples. Artificial neural network (ANN) is a structure imitating the learning path of the human brain; learning, remembering, generalizing, basic functions such as generating new data from the data collected by generalization. ANN is an information processing structure which inspired by biological nervous systems, such as the human brain. Typically, an ANN consists of three main layers, each of which has several interconnected parallel processing units, called neurons (shortly nodes). These are the input layer, the output layer, and between them the hidden layers that can consist of one or more layers [35]. ANN learns the relation between input and output variables by examining (training) the previously recorded data. Basically, from incoming connections, a neuron takes input and combines the input, usually performs a non-linear operation, and then finally outputs the results [36-38]. An ANN involves multiple layers of some processing units called neurons. These neurons perform two functions which are the collection of inputs and the generation of an output. This ANN can be used to decide the learning type to adjust the weights with changes in parameters [39]. When constructing a functional model of the biological neuron, there are three essential components. First, the synapses of the neuron modeled by weight. The strength of the connection between an input and a neuron is specified by the value of the weight. Negative weight values reflect inhibitory links, while positive values indicate stimulating links. The next two components model the actual activity within the neuronal cell. An aggregator summarizes all altered entries based on their respective weight. This activity is called linear combination. Finally, an activation function controls the amplitude of the neuron's output, where an acceptable range of output is usually between 0 and 1 or between -1 and 1. ANN is an intensive tool to solve many problems due to its features such as nonlinearity, information processing, learning and adaptation. There are two main categories of neural network architecture depending on the type of connections between neurons, forward neural networks and recurrent neural networks. If there is no feedback across the network from the outputs of the neurons to the inputs, the network is called a feed forward neural network. Feed forward neural networks are divided into two categories depending on the number of layers, single layer or multilayer. The Multilayer Perceptrons (MLPs) model is a type of neural network [40]. MLP is known as a class of feed forward artificial neural network (ANN) [41]. MLPs models are basic deep neural networks and consist of a series of fully connected layers. Each new layer is a nonlinear function of the weighted sum of all outputs from the previous one. MLP machine learning methods are used to meet the high computing power requirements of modern deep learning architectures. MLP has a supervised learning technique called backpropagation for training [42,43]. MLPs are suitable for tabular

datasets, classification prediction problems and regression prediction problems. Deep neural network (DNN) model is a powerful machine learning and artificial intelligence tool. A deep neural network (DNN) is a multilayer artificial neural network (ANN) between the input and output layers. DNN is used to model complex nonlinear relationships. "Deep" is used to refer to functions that are more complex in terms of the number of layers and units in a single layer. Creating more accurate models using additional and larger layers makes it possible to capture higher-level patterns in large data sets [44-47]. One type of the popular of DNN is Multi-Layer Perceptrons (MLPs) [48].

2.3.1 Evaluation metrics

Model performance evaluation for The Estimation of dose rates have been conducted using accuracy. Statistical metrics are used to evaluate the results of prediction models and to compare these models with each other [49]. MSE (Mean Squared Error), RMSE (Root Mean Squared Error), MAE (Mean absolute error) and R^2 (R-Squared) metrics can be expressed as below equations (1-4). In the formulas, n, actual, estimated, $\overline{actual}$ and $\overline{estimated}$ are the number of data, the actual values, the estimated values, the mean of the actual values and the mean of the estimated values, respectively.

$$MSE = \frac{1}{n}\sum_{i=1}^{n}(actual_i - estimate\,d_i)^2 \quad (1)$$

$$RMSE = \sqrt{\frac{1}{n}\sum_{i=1}^{N}(actual_i - estimated_i)^2} \quad (2)$$

$$MAE = \frac{1}{n}\sum_{i=1}^{n}|actual_i - estimated_i| \quad (3)$$

$$R^2 = 1 - \frac{\sum_{i=1}^{n}(actual_i - estimate\,d_i)^2}{\sum_{i=1}^{n}(actual_i - \overline{actual})^2} \quad (4)$$

2.3.2 Datasets

Thirty-six different domestic flights relating to Istanbul and Ankara Airports in Turkey were investigated. Detailed record of a flight's location and flight data obtained from Flightradar24 [50]. In the CARI-7A program, the instantaneous dose rate during the flight and the total effective dose were calculated by using the flight time, latitude, longitude and altitude values. A total of 3057 instances and 4 attributes were used in the process of developing models with each machine learning method used. Cosmic radiation dose estimation via machine learning was done by (MLPs). Latitude, longitude and depth were used as inputs to the developed models, and target is the dose rate. ReLu (Rectified Linear Unit), hyperbolic tangent and logistic sigmoidal were used as activation functions. A stratified k-cross validation approach (k=5,10 and 20) and random

sampling approach (training set size is 66%) were used for splitting the dataset into train data and test data to develop a MLPs model. The models were evaluated using four indicators: MSE (Mean Squared Error), RMSE (Root Mean Squared Error), MAE (Mean absolute error) and R^2 (R-Squared).

3. Results

A Deep Neural Networks (DNNs) and CARI-7A program was used to calculate the effective dose form cosmic radiation for 36 domestic flights in Turkey. Additionally, percentage contribution of the dose from each particle to the total dose for the domestic flights were calculated. Percentage contribution of the dose from each particle are given in Appendix 1. Route data were obtained from the Flight24 site to calculate the effective doses received for 36 selected domestic flights. These data are: ascending and descending time, flight levels and flight time, origin and destination airports at each level information for each flight. Flight times vary between 48 and 127 minutes for domestic flights related with Ankara and Istanbul Airport. In this study, Deep Neural Networks (DNNs) via Multilayer Perceptrons (MLPs) were used to estimate the radiation doses due to cosmic radiation for different domestic flights. For 36 flights, Multilayer Perceptrons results details (number of cross validations, name of the activation function, number of hidden layers etc...) and evaluation metrics results are presented in Table 1. Four metrics were used to evaluate the accuracy of the MLPs model. In MLP method 3 different activation function used for the calculated effective doses: hyperbolic tangent, logistic sigmoidal, Rectified Linear Unit (RELU). When Table 1 examined, it is seen that the best result was obtained for Model 27. In addition, when learning time and testing time are taken into account, the closest results to Model 27 were obtained in Model 2. These results were marked as bold in Table 1. CARI-7A program was another method used in this study. CARI-7A is a program that calculates the effective radiation doses received by the passengers and aircrew members during flight. The program requires user input such as attitude, longitude, altitude, flight duration time, the date of the flight, geographic locations of starting airports and geographic locations of landing airports. Result of calculation 27 and CARI-7A for the domestic flights are given in Table 2. In Table 2, it is seen that the effective dose values calculated for one-way flights for both methods ranged from 0.3 μSv to 3.5 μSv. The effective dose results obtained for each flight one by the code CARI-7A are presented as a histogram in at Appendix 2. It can be seen that MLPs method and CARI-7A are in good agreement in Table 2.

Another important parameter in calculating the dose value in flights is the latitude parameter. The view of effective dose rate values against latitude and depth parameters is presented in Fig. 1. The results of two separate methods used

to calculate the effective dose are shown in Fig. 2. Fig. 3 shows the comparison of effective doses calculated for maximum and minimum of solar cycles.

Table 1

Summary of Multilayer Perceptrons (MLPs) calculation and metrics.

Model	Number of hidden layers	Number of neurons per each hidden layer	Activation function	Sampling	Train time	Test time	Metrics			
							MSE	RMSE	MAE	R^2
1	5	65	ReLu	5-Cross validation	20.275	0.081	0.001	0.028	0.016	0.999
2	**5**	**65**	**ReLu**	**10-Cross validation**	**44.321**	**0.105**	**0.000**	**0.017**	**0.011**	**1.000**
3	5	65	ReLu	20-Cross validation	93.952	0.130	0.000	0.019	0.011	1.000
4	5	65	ReLu	Random	52.559	0.118	0.000	0.017	0.011	1.000
5	5	65	tanh	5-Cross validation	18.904	0.074	0.000	0.020	0.015	1.000
6	5	65	tanh	10-Cross validation	58.428	0.114	0.000	0.018	0.013	1.000
7	5	65	tanh	20-Cross validation	98.993	0.142	0.000	0.019	0.014	1.000
8	5	65	tanh	Random	48.007	0.101	0.000	0.018	0.013	1.000
9	5	65	logistic	5-Cross validation	53.418	0.098	0.002	0.039	0.024	0.999
10	5	65	logistic	10-Cross validation	118.646	0.102	0.001	0.036	0.022	0.999
11	5	65	logistic	20-Cross validation	194.924	0.125	0.001	0.038	0.022	0.999
12	5	65	logistic	Random	116.031	0.091	0.001	0.036	0.022	0.999
13	5	100	ReLu	5-Cross validation	30.495	0.145	0.001	0.027	0.015	0.999
14	5	100	ReLu	10-Cross validation	95.746	0.201	0.000	0.017	0.010	1.000
15	5	100	ReLu	20-Cross	148.111	0.188	0.000	0.021	0.012	1.000

				validation						
16	5	100	ReLu	Random	57.603	0.136	0.000	0.017	0.010	1.000
17	5	100	tanh	5-Cross validation	26.281	0.104	0.000	0.022	0.016	1.000
18	5	100	tanh	10-Cross validation	50.419	0.110	0.000	0.021	0.014	1.000
19	5	100	tanh	20-Cross validation	101.585	0.137	0.000	0.020	0.013	1.000
20	5	100	tanh	Random	65.291	0.133	0.000	0.021	0.014	1.000
21	5	100	logistic	5-Cross validation	89.613	0.119	0.001	0.034	0.022	0.999
22	5	100	logistic	10-Cross validation	160.738	0.127	0.001	0.031	0.019	0.999
23	5	100	logistic	20-Cross validation	394.692	0.270	0.001	0.032	0.019	0.999
24	5	100	logistic	Random	145.656	0.132	0.001	0.031	0.019	0.999
25	5	150	ReLu	5-Cross validation	39.491	0.161	0.000	0.014	0.008	1.000
26	5	150	ReLu	10-Cross validation	83.475	0.240	0.000	0.014	0.008	1.000
27	**5**	**150**	**ReLu**	**20-Cross validation**	**170.323**	**0.248**	**0.000**	**0.013**	**0.008**	**1.000**
28	5	150	ReLu	Random	77.934	0.186	0.000	0.014	0.008	1.000
29	5	150	tanh	5-Cross validation	43.456	0.140	0.002	0.048	0.037	0.998
30	5	150	tanh	10-Cross validation	85.791	0.177	0.001	0.025	0.019	1.000
31	5	150	tanh	20-Cross validation	195.298	0.242	0.001	0.034	0.027	0.999
32	5	150	tanh	Random	96.674	0.184	0.001	0.025	0.019	1.000
33	5	150	logistic	5-Cross validation	93.371	0.154	0.001	0.029	0.019	0.999
34	5	150	logistic	10-Cross validation	189.472	0.170	0.001	0.028	0.019	0.999
35	5	150	logistic	20-Cross validation	395.112	0.222	0.001	0.028	0.018	0.999
36	5	150	logistic	Random	259.505	0.241	0.001	0.028	0.019	0.999

37	5	200	ReLu	5-Cross validation	80.163	0.365	0.000	0.016	0.010	1.000
38	5	200	ReLu	10-Cross validation	131.773	0.276	0.000	0.014	0.008	1.000
39	5	200	ReLu	20-Cross validation	315.987	0.346	0.001	0.027	0.012	1.000
40	5	200	ReLu	Random	315.987	0.346	0.001	0.027	0.012	1.000
41	5	200	tanh	5-Cross validation	138.267	0.287	0.001	0.033	0.024	0.999
42	5	200	tanh	10-Cross validation	132.749	0.218	0.001	0.035	0.027	0.999
43	5	200	tanh	20-Cross validation	225.221	0.263	0.001	0.030	0.024	0.999
44	5	200	tanh	Random	131.164	0.219	0.001	0.035	0.027	0.999
45	5	200	logistic	5-Cross validation	140.166	0.185	0.001	0.038	0.024	0.999
46	5	200	logistic	10-Cross validation	1905.378	1.797	0.001	0.035	0.021	0.999
47	5	200	logistic	20-Cross validation	2786.237	1.316	0.001	0.031	0.019	0.999
48	5	200	logistic	Random	229.509	0.160	0.001	0.035	0.021	0.999

Table 2

Effective Dose (μSv) obtained by Model 27 and CARI-7A for the domestic flights.

Domestic Flights											
Flight	Departure	Destination	Fligt date	Fligt time (minutes)	CARI-7A (flight date)	MLPs (Calculation 27)	Solar cycle 23 (minimum) 1996-08	Solar cycle 23 (maximum) 2001-11	Solar cycle 24 (minimum) 2008-12	Solar cycle 24 (maximum) 2014-4	Solar cycle 25 (minimum) 2019-12
					Effective Dose (μSv)						
1	Adana	Ankara	2020-12-21	70	0.7	0.7	0.6	0.6	0.7	0.6	0.7
2	Adana	Istanbul	2020-12-18	102	1.8	1.8	1.7	1.6	1.8	1.7	1.8
3	Ankara	Istanbul	2020-12-17	74	0.5	0.5	0.5	0.5	0.5	0.5	0.5

4	Ankara	Istanbul	2020-12-19	59	0.5	0.5	0.5	0.4	0.5	0.4	0.5
5	Ankara	Izmir	2020-12-17	72	1.2	1.2	1.2	1.1	1.3	1.2	1.3
6	Antakya	Istanbul	2020-12-21	127	2.8	2.8	2.7	2.5	2.8	2.6	2.8
7	Antalya	Ankara	2020-12-21	64	0.7	0.7	0.7	0.6	0.7	0.7	0.7
8	Antalya	Istanbul	2020-12-19	68	0.9	0.9	0.8	0.8	0.9	0.8	0.9
9	Canakkale	Ankara	2020-12-23	54	1.1	1.1	1.1	1.0	1.2	1.1	1.2
10	Dalaman	Ankara	2020-12-20	53	1.4	1.4	1.4	1.3	1.4	1.3	1.4
11	Dalaman	Istanbul	2020-12-18	75	1.5	1.6	1.5	1.4	1.5	1.4	1.5
12	Antalya	Istanbul	2020-12-18	73	1.0	1.0	1.0	0.9	1.1	1.0	1.1
13	Gaziantep	Istanbul	2020-12-14	80	3.0	3.0	3.0	2.7	3.1	2.8	3.1
14	Igdir	Ankara	2020-12-21	107	3.3	3.2	3.1	2.9	3.3	3.0	3.3
15	Istanbul	Ankara	2020-12-21	48	0.6	0.6	0.6	0.5	0.6	0.6	0.6
16	Izmir	Ankara	2020-12-22	68	1.1	1.1	1.0	0.9	1.1	1.0	1.1
17	Izmir	Istanbul	2020-12-19	60	0.3	0.3	0.3	0.3	0.3	0.3	0.3
18	Izmir	Ankara	2020-12-21	55	1.2	1.2	1.2	1.1	1.2	1.1	1.2
19	Istanbul	Antalya	2020-12-18	57	0.9	0.9	0.9	0.8	0.9	0.9	0.9
20	Istanbul	Ankara	2020-12-18	51	0.6	0.6	0.6	0.6	0.6	0.6	0.6
21	Istanbul	Izmir	2020-12-17	63	0.5	0.5	0.5	0.5	0.5	0.5	0.5
22	Istanbul	Antalya	2020-12-18	70	1.1	1.1	1.0	0.9	1.1	1.0	1.1
23	Istanbul	Adana	2020-12-18	72	1.7	1.7	1.7	1.5	1.8	1.6	1.8
24	Istanbul	Bodrum	2020-12-14	58	1.1	1.1	1.1	1.0	1.1	1.0	1.1
25	Istanbul	Dalaman	2020-12-20	54	0.8	0.8	0.8	0.7	0.8	0.8	0.8
26	Istanbul	Trabzon	2020-12-18	80	2.9	2.9	2.8	2.5	2.9	2.7	2.9
27	Kahramanmaras	Ankara	2020-12-21	48	0.9	0.9	0.9	0.8	0.9	0.9	0.9
28	Kars	Ankara	2020-12-18	75	2.8	2.8	2.7	2.5	2.9	2.6	2.9
29	Kayseri	Istanbul	2020-12-23	82	1.6	1.6	1.5	1.4	1.6	1.5	1.6
30	Amasya	Istanbul	2020-12-25	69	1.8	1.8	1.8	1.6	1.9	1.7	1.9
31	Nevsehir	Istanbul	2020-12-16	62	1.3	1.3	1.3	1.2	1.3	1.2	1.3
32	Samsun	Ankara	2020-12-22	54	0.5	0.5	0.5	0.4	0.5	0.5	0.5
33	Samsun	Istanbul	2020-12-23	88	1.3	1.3	1.2	1.1	1.3	1.2	1.3
34	Trabzon	Ankara	2020-12-21	58	1.9	1.9	1.9	1.7	2.0	1.8	2.0
35	Trabzon	Ankara	2020-12-22	70	1.7	1.7	1.6	1.5	1.7	1.6	1.7
36	Trabzon	Istanbul	2020-12-20	100	3.5	3.4	3.3	3.0	3.5	3.2	3.5

The view of effective dose rate values against latitude and depth parameters is presented in Fig 1.

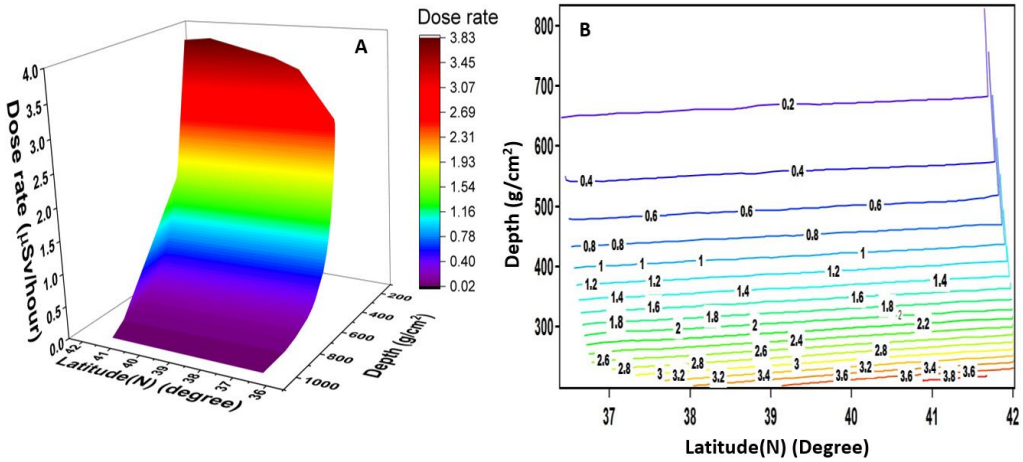

Fig. 1. A) 3-dimensional view of effective dose rates depending on latitude and depth. B) Projection of 3-dimensional surface

The results of two separate methods used to calculate the effective dose are shown in Figure 2. Figure 3 shows the comparison of effective doses calculated for maximum and minimum of solar cycles.

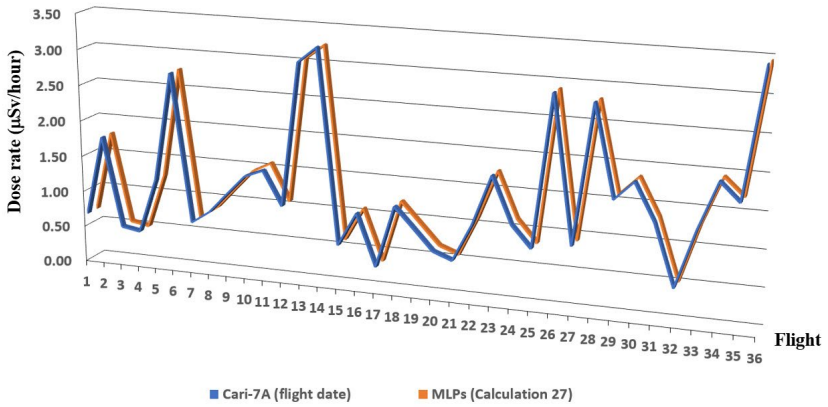

Fig. 2. Comparison of the calculated effective

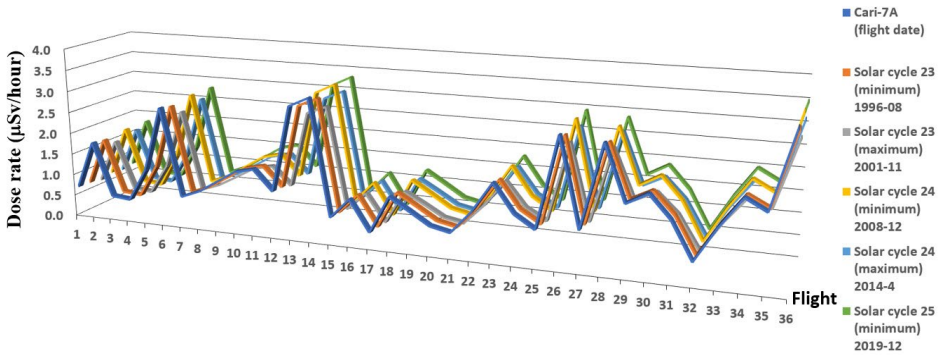

Fig. 3. Comparison of effective doses calculated for maximum and minimum of solar cycles

4. Conclusion

Cosmic radiation doses received on aboard an aircraft are higher than on the ground level. Aircrew can receive an effective dose of several millisievert per year as a result of their occupation. It is important for frequent flyers and flight crew members to monitor the dose values they receive and adjust the flight frequency accordingly in order to reduce the health risks that may occur. In this present study, effective dose values from cosmic radiation were calculated with CARI-7A and DNN. This study has proposed that machine learning method and different algorithms could be used to evaluate cosmic radiation dose received during a flight. The calculated dose values obtained by the CARI-7A program and the models developed by the DNN were compared and seen that they were in good agreement. As a result, DNN approach is a useful and powerful tool for estimation of the effective dose values.

REFERENCES

[1]. *Cosmic Radiation: Why We Should Not Be Worried.* 12 Nisan 2021, https://www.iaea.org/newscenter/news/cosmic-radiation-why-we-should-not-be-worried.

[2*J. D. T. Bartlett*, "Radiation protection aspects of the cosmic radiation exposure of aircraft crew", Radiation Protection Dosimetry, **Volume 109**, Issue 4, Pages 349–355, July 2004.

[3]. *M. Bagshaw*, "Cosmic radiation in commercial aviation", Travel Medicine and Infectious Disease, **Volume 6**, Issue 3, Pages 125-127, May 2008.

[4]. COUNCIL DIRECTIVE 2013/59/EURATOM laying down basic safety standards for protection against the dangers arising from exposure to ionising radiation, Published on 6 June 2017. Last updated on 23 September 2020.

[5]. Cosmic Radiation Exposure of Aircraft Crew, EUROPEAN COMMISSION, Radiation Protection 140 https://ec.europa.eu/energy/sites/ener/files/documents/140.pdf. (Accessed January 2, 2021).

[6]. European Commission, No 173, Comparison of codes assessing radiation exposure of aircraft crew due to galactic cosmic radiation, ISSN 1681-6803.

[7]. *M. Latocha*, *P. Beck* and *S. Rollet*, "AVIDOS – a software package for European accredited aviation dosimetry", Radiat.Prot.Dosimetry, **136**(4) 286-290 (2009).

[8]. *Kyle Copeland*, "CARI-7A: DEVELOPMENT AND VALIDATION", Radiation Protection Dosimetry, **Volume 175**, Issue 4, Pages 419–431, August 2017, https://doi.org/10.1093/rpd/ncw369

[9]. V. Mares, et al., "Air crew dosimetry with a new version of EPCARD", Radiat. Prot. Dosim. **Vol. 136**, No. 4, pp. 262-266. (2009).

[10]. *F. Wissmann*, "Long-term measurements of H*(10) at aviation altitudes in the northern hemisphere", Radiat. Prot. Dosim. **121**(4), 347-357 (2006).

[11]. *Hiroshi Yasuda*, *Tatsuhiko Sato* and *Masato Terakado*, "A Personal Use Program for Calculation of Aviation Route Doses", IRPA12 Congress,(2008).

[12]. *B. Levis*, *M. Desormeaux*, et al., "Assessment of Aircrew Radiation Exposure by further measurements and model development", Radiation protection dosimetry (2004). 111. 151-71. 10.1093/rpd/nch333.

[13]. *Tatsuhiko Sato*, "EXPACS: Excel-based Program for calculating Atmospheric Cosmic-ray Spectrum User's Manual." (2016).

[14]. *J. F. Bottollier-Depois*, *P. Blanchard*, *I. Clairand*, *P. Dessarps*, *N. Fuller*, *P. Lantos*, *D. Saint-Lô*, *F. Trompier*, "An operational approach for aircraft crew dosimetry: the SIEVERT system", Radiation Protection Dosimetry, **Volume 125**, Issue 1-4, July 2007, Pages 421–424, https://doi.org/10.1093/rpd/ncl555

[15]. *A. Ferrari*, *M. Pelliccioni*, and *T. A. Rancati*, "Method Applicable to Effective Dose Rate Estimates for Aircrew Dosimetry", Radiation Protection Dosimetry, **96**(1-3):219-222 (2001), doi: 10.1093/oxfordjournals.rpd.a006586.

[16]. *A. Ferrari*, *M. Pelliccioni*, and *R. A. Villari*, "Mathematical Model of Aircraft for Evaluating the Effects of Shielding Structure on Aircrew Exposure", Radiation Protection Dosimetry, **116**(1– 4):331–335 (2005), doi: 10.1093/rpd/nci144.

[17]. *W. Friedberg*, *F. E. Duke*, *L. Snyder*, *D. N. Faulkner*, et al, "The Cosmic Radiation Environment at Air Carrier Flight Altitudes and Possible Associated Health Risks", Radiation Protection Dosimetry. **48**(1): 21–25 (1993).

[18]. *B. J. Lewis*, et al, "Aircrew Exposure from Cosmic Radiation on Commercial Airline Routes.", Radiation Protection Dosimetry, **93**(4):293–314. (2001), https://doi.org/10.1016/j.enconman.2007.09.021

[19]. *L. Amon Susam*, et al., "Cosmic Radiation Exposure Calculations for International And Domestic Flights Departs From Istanbul And Ankara", Radiation Protection Dosimetry, **192**(1): 61-68 (2020). https://doi.org/10.1093/rpd/ncaa182

[20]. *M. Daniel*, *M.M. Matthias* and *R. Günther*, "Numerical calculation of the radiation exposure from galactic cosmic rays at aviation altitudes with the PANDOCA core model.", (2014), https://doi.org/10.1002/2013SW001022

[21]. CARI-7 Documentation: User's Guide, https://www.faa.gov/data_research/research/med_humanfacs/oamtechreports/2020s/media/202106.pdf (Accessed December 20, 2020).

[22]. *J. H. Jr Adams*, *S. Heiblim* and *C. Malott*, "Evaluation of galactic cosmic ray models, presented at IEEE "Nucl. Space Radiat. Effects Conf., Quebec City, QC, Can, July 2009. Available at: https://ntrs.nasa.gov/search.jsp?N=0&Ntk=All&Ntt=20090034942&Ntx=mode%20matchallpartial&Nm=123|Collection|NA SA%20STI||17|Collection|NACA

[23]. International Standards Organization Space Environment (Natural and Artificial) – Galactic Cosmic Ray Model (ISO 15930:2004) (Geneva, Switzerland: ISO) (2004).

[24]. *P. O'Neill*., *M. Badhwar–O'Neill*, "Galactic cosmic ray flux model—revised.", IEEE Trans. Nucl. Sci. **57**(6), 3148–3153 (2010) 10.1109/TNS.2010.2083688.

[25]. *K. Herbst*, *A. Kopp*, *B. Heber*, et al., "On the importance of the local interstellar spectrum for the solar modulation parameter", J. Geophys. Res., **115**, D00I20 (2010), doi:10.1029/2009JD012557.

[26]. The 2007 Recommendations of the International Commission on Radiological Protection, ICRP Publication 103. Ann. ICRP 37 (2-4), ICRP (2007).

[27]. *Mitchell Tom*, "Machine Learning. New York: McGraw Hill.", (1997), ISBN 0-07-042807-7. OCLC 36417892.

[28]. "What is Machine Learning?", www.ibm.com. Retrieved 2021-08-15.

[29]. *Stuart Jonathan*, "Artificial Intelligence : a Modern Approach. Upper Saddle River, N.J. :Prentice Hall, 2010.

[30]. *Fabian Pedregosa* et al.," Scikit-learn: Machine Learning in Python", JMLR **12**, pp. 2825-2830, 2011.

[31]. *C.R. Harris*, *K.J. Millman*, et al. "Array programming with NumPy"., Nature **585**, 357–362 (2020). DOI: 10.1038/s41586-020-2649-

[32]. *J. D. Hunter*, "Matplotlib: A 2D Graphics Environment", Computing in Science & Engineering, **vol. 9**, no. 3, pp. 90-95, 2007.

[33]. *Pauli Virtanen, Ralf Gommers*, *Travis E. Oliphant*, *Matt Haberland*, *Tyler Reddy*, *David Cournapeau*, *Evgeni Burovski*, *Pearu Peterson*, *Warren Weckesser*, *Jonathan Bright*, *Stéfan J. van der Walt*, *Matthew Brett*, *Joshua Wilson*, *K. Jarrod Millman*, *Nikolay Mayorov*, *Andrew R. J. Nelson*, *Eric Jones*, *Robert Kern*, *Eric Larson*, *CJ Carey*, *İlhan Polat*, *Yu Feng*, *Eric W. Moore*, *Jake VanderPlas*, *Denis Laxalde*, *Josef Perktold*, *Robert Cimrman*, *Ian Henriksen*, *E.A. Quintero*, *Charles R Harris*, *Anne M. Archibald*, *Antônio H. Ribeiro*, *Fabian Pedregosa*, *Paul van Mulbregt* and SciPy 1.0 Contributors. (2020) SciPy 1.0: Fundamental Algorithms for Scientific Computing in Python. Nature Methods, 17(3), 261-272.

[34]. *K Sushilkumar*, "Analysis of WEKA Data Mining Algorithm REPTree, Simple Cart and RandomTree for Classification of Indian News", IJISET - International Journal of Innovative Science, Engineering & Technology, **Vol. 2,** Issue 2, ISSN 2348 – 7968 (2015).

[35]. *V. Vasif NABIYEV*, "Yapay Zeka", Seçkin Yayıncılık, Ankara (2003).

[36]. N. Gilles, et al. Some Applications of ANN to Solar Radiation Estimation and Forecasting for Energy Applications, Appl. Sci. 2019, **9**(1), 209. (2019), https://doi.org/10.3390/app9010209

[37]. *C. Gurlek* and *M. Sahin*, "Estimation of the Global Solar Radiation with the Artificial Neural Networks for the City of Sivas", European Mechanical Science. **Vol. 2**(2): 46-51 (2018). https://doi.org/10.26701/ems.359681

[38]. *O. Görler* and *S. Akkoyun*, "Artificial Neural Networks Can be Used as Alternative Method to Estimate Loss Tooth Root Sizes for Prediction of Dental Implants,", C.U. Faculty of Science Science Journal. 38, 1300-1949 (2017). DOI: 10.17776/cumuscij.304902

[39]. *C. J. Lam*, *K. K. W. Wan* and *L. Yang*, "Solar Radiation Modelling Using Anns for Different Climates in China, **vol.49**, pp.1080-1090 (2008). https://doi.org/10.1016/j.enconman.2007.09.021

[40]. *A. D. Dongare*, *D. D. Kharde* and *D. K. Amit*, "Introduction to Artificial Neural Network", International Journal of Engineering and Innovative Technology (IJEIT) 2:(1), ISSN: 2277-3754 (2012).

[41]. *Trevor Hastie*, Tibshirani, Robert. Friedman, Jerome, "The Elements of Statistical Learning: Data Mining, Inference, and Prediction.", Springer, New York, NY, 2009.

[42]. Rosenblatt, Frank, "Principles of Neurodynamics: Perceptrons and the Theory of Brain Mechanisms.", Spartan Books, Washington DC, 1961.

[43]. *David E. Rumelhart*, *E. Hinton Geoffrey* and *R. J. Williams*, "Learning Internal Representations by Error Propagation". David E. Rumelhart, James L. McClelland, and the PDP research group. (editors), Parallel distributed processing: Explorations in the microstructure of cognition, Volume 1: Foundation. MIT Press, 1986.

[44]. *C. M. Bishop*, "Pattern Recognition and Machine Learning.", Chapter 5: Neural Networks (2006).

[45]. *J. Schmidhuber*, "Deep Learning in Neural Networks: An Overview.", Neural Networks **61**, 85-117, (2015).

[46]. *Y. Bengio*, et al., "Deep Learning.", Nature **521**: 436-44 (2015).

[47]. *I. Goodfellow*, *Y. Bengio* and *A. Courville*, "Deep Learning", MIT Press. (2016).

[48]. *Wesam Salah Alaloul* and *Abdul Hannan Qureshi* (May 26th 2020), "Data Processing Using Artificial Neural Networks," Dynamic Data Assimilation - Beating the Uncertainties, edit by Dinesh G. Harkut, Intech Open, DOI: 10.5772/intechopen.91935. Available from: https://www.intechopen.com/chapters/71673

[49]. *X.N. Bui*, et al., "Developing a predictive method based on optimized M5Rules–GA predicting heating load of an energy- efcient building system", Engineering with Computers **36**:931–940 (2020). https://doi.org/10.1007/s00366-019-00739-8

[50]. https://www.flightradar24.com/39.92,32.86/8 (Accessed December 2, 2020 – January 20, 2021)

Appendix 1

Percentage contribution of the dose from each particle to the total dose

Flight	NEUTRONS	PHOTONS	ELECTRONS	POSITRONS	NEGATIVE MUONS	POSITIVE MUONS	PROTONS	NEGATIVE PIONS	POSITIVE PIONS	DEUTERONS	TRITONS	HELIONS	ALPHAS
1	45.1	17.0	10.3	4.5	4.3	4.3	13.8	0.1	0.1	0.2	0.0	0.1	0.2
2	43.3	17.8	11.2	5.0	3.3	3.3	14.8	0.1	0.1	0.3	0.0	0.2	0.4
3	48.5	15.2	8.9	3.9	4.6	4.6	13.6	0.1	0.1	0.2	0.0	0.1	0.1
4	49.3	14.9	8.6	3.8	4.6	4.6	13.5	0.1	0.1	0.2	0.0	0.1	0.1
5	44.4	17.4	10.8	4.8	3.4	3.4	14.7	0.1	0.1	0.3	0.0	0.2	0.3
6	41.4	18.4	12.0	5.3	3.0	3.0	15.3	0.1	0.1	0.3	0.0	0.3	0.6
7	44.3	17.3	10.7	4.7	4.0	4.0	14.2	0.1	0.1	0.3	0.0	0.2	0.3
8	44.9	17.1	10.5	4.6	3.8	3.8	14.3	0.1	0.1	0.3	0.0	0.2	0.3
9	45.7	16.8	10.4	4.6	3.3	3.3	15.0	0.1	0.1	0.3	0.0	0.2	0.3
10	41.2	18.1	12.0	5.3	2.9	2.9	15.7	0.1	0.1	0.3	0.0	0.4	0.8
11	42.8	16.8	10.7	4.7	4.7	4.7	14.4	0.1	0.1	0.3	0.0	0.3	0.4
12	44.7	17.3	10.6	4.7	3.8	3.8	14.2	0.1	0.1	0.3	0.0	0.2	0.3
13	42.4	17.8	11.6	5.1	2.6	2.6	16.0	0.1	0.1	0.3	0.0	0.4	0.7
14	43.2	17.4	11.3	5.0	2.7	2.7	16.0	0.1	0.1	0.3	0.0	0.4	0.6
15	49.0	15.3	9.0	3.9	4.1	4.1	13.8	0.1	0.1	0.3	0.0	0.1	0.1
16	44.2	17.4	10.9	4.8	3.5	3.5	14.6	0.1	0.1	0.3	0.0	0.2	0.3
17	48.5	14.8	8.6	3.8	5.4	5.4	12.8	0.1	0.1	0.2	0.0	0.1	0.1
18	42.7	17.7	11.4	5.0	3.1	3.1	15.3	0.1	0.1	0.3	0.0	0.3	0.6
19	45.5	17.0	10.4	4.6	3.6	3.6	14.3	0.1	0.1	0.3	0.0	0.2	0.2
20	47.3	16.0	9.6	4.2	3.8	3.8	14.4	0.1	0.1	0.3	0.0	0.2	0.2
21	49.5	14.9	8.5	3.8	4.7	4.7	13.2	0.1	0.1	0.2	0.0	0.1	0.1
22	44.5	16.0	9.7	4.3	5.7	5.7	13.2	0.1	0.1	0.2	0.0	0.2	0.2
23	44.5	17.3	10.9	4.8	3.1	3.1	15.1	0.1	0.1	0.3	0.0	0.2	0.4
24	43.7	17.2	11.0	4.8	3.2	3.2	15.3	0.1	0.1	0.3	0.0	0.3	0.5
25	45.2	17.1	10.5	4.6	3.8	3.8	14.2	0.1	0.1	0.3	0.0	0.2	0.2
26	44.4	16.5	10.7	4.7	2.6	2.6	16.6	0.1	0.1	0.3	0.0	0.4	0.7
27	44.4	17.5	10.8	4.8	3.5	3.5	14.5	0.1	0.1	0.3	0.0	0.2	0.3
28	42.6	17.4	11.5	5.0	2.6	2.6	16.2	0.1	0.1	0.3	0.0	0.4	0.8
29	45.7	16.9	10.4	4.6	3.3	3.3	14.8	0.1	0.1	0.3	0.0	0.2	0.3
30	45.2	16.8	10.6	4.7	3.0	3.0	15.5	0.1	0.1	0.3	0.0	0.3	0.4
31	44.8	17.0	10.7	4.7	3.2	3.2	15.2	0.1	0.1	0.3	0.0	0.3	0.4
32	49.9	14.8	8.5	3.7	4.6	4.6	13.4	0.1	0.1	0.2	0.0	0.1	0.1
33	47.8	15.9	9.5	4.2	3.6	3.6	14.5	0.1	0.1	0.3	0.0	0.2	0.2
34	44.1	17.0	11.0	4.8	2.7	2.7	16.0	0.1	0.1	0.3	0.0	0.4	0.6
35	46.0	16.7	10.3	4.5	3.1	3.1	15.2	0.1	0.1	0.3	0.0	0.2	0.3
36	43.2	16.9	11.2	4.9	2.6	2.6	16.6	0.1	0.1	0.3	0.0	0.5	0.8
MEAN	45.1	16.8	10.4	4.6	3.6	3.6	14.7	0.1	0.1	0.3	0.0	0.2	0.4
SD(σ)	2.3	1.0	1.0	0.4	0.8	0.8	1.0	0.0	0.0	0.0	0.0	0.1	0.2

Appendix 2

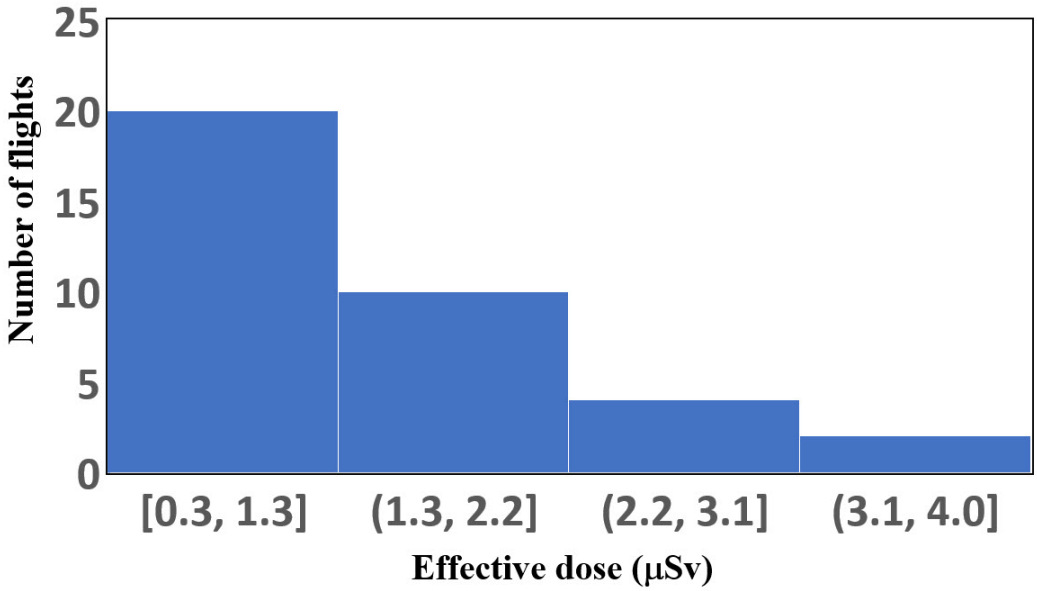

Frequency distribution of the effective dose values according to the number